

Subproject C1.05

**Oxo / Hydroxo Clusters of the Lanthanides for Potential
Photonic and Magnetic Applications**

Principal Investigator: Peter W. Roesky

CFN-Financed Scientists: Asamanjoy Bhunia (1/2 E13, since Feb. 2008), Matthias Schmid (January 2010 – March 2010), Pavel Petrov (April 2010 – Mai 2010), Dr. Sebastian Marks (since May 2010).

Further Scientists: Dominique T. Thielemann, Dr. Balasubramanian Murugesapandian.

**Institut für Anorganische Chemie
Karlsruher Institut für Technologie (KIT)**

Oxo / Hydroxo Clusters of the Lanthanides for Potential Photonic and Magnetic Applications

Introduction

During the last decade, metal–organic frameworks (MOFs) and infinite coordination polymers (ICPs) have attracted the attention of a huge number of chemists [1-5]. The reasons for this are the enormous variety of interesting molecular-based topologies as well as the potential variety of properties, with promising applications such as the storage of gases [6], catalysis [7], and sensors for special classes of molecules [8]. Some of these materials also show excellent physical properties such as magnetism [9], luminescence [10, 11], and optoelectronic effects [12].

Coordination oligomers (clusters) also continue to attract considerable attention because they represent the bridge linking molecular and solid state chemistry. They are useful tools for understanding the size-dependent physical properties of electronic materials. While the cluster chemistry of the *d*-block transition metals is firmly established and huge clusters have been isolated, the analogous chemistry of the lanthanides is less developed [13, 14]. The lanthanide ions generally display variable and high coordination numbers and the energy difference between the various coordination numbers is small. Therefore, the use of lanthanide ions for the construction of coordination polymers and clusters is more difficult than their *d*-block metal analogues. Lanthanide clusters are known to feature two potentially useful physical properties: luminescence and magnetism.

a) Luminescence

Emission of light from lanthanide ions is a fundamentally important process with a continuously expanding field of applications in contemporary electronic devices, ranging from TV screens to lasers and optical fibers. While the introduction of lanthanides into solid state oxide materials has hitherto shown to be facile, the incorporation of *e.g.* NIR-emissive lanthanide ions into emerging materials like *e.g.* organic polymers remains challenging due to the intrinsic properties of lanthanide sources and the various technological barriers associated with solids processing. Lanthanide cluster compounds with their solubility in organic solvents and their relatively high concentration of lanthanide ions/unit volume are promising sources of lanthanide ions in the preparation of emissive composite materials [15].

b) Magnetism

The study of paramagnetic metal ion clusters has been of increasing interest since such compounds have shown to exhibit magnetic memory effects. In fact, depending on the nature of these aggregates, they can behave as Single-Molecule-Magnets (SMM) [16-19]. Most of the previous studies were largely based on *d*-block transition metal compounds. The incorporation of lanthanides into these clusters has been investigated to take advantage of the potentially large number of unpaired *f*-electrons available. However, there are very few pure aggregates of lanthanide elements reported. Controlling the synthesis and understanding the properties of these unique structures ought to have an impact on the future manufacture of nanodevices based on electronic, magnetic or optical properties related to well-defined molecular units.

c) Synthesis

Lanthanide oxo/hydroxo clusters [13, 20] attract significant attention because they have proven to be useful for a variety of applications ranging from luminescent [21-23] to magnetic materials [24-26]. They have also been used in homogeneous catalysis [27]. Although this field of research is still

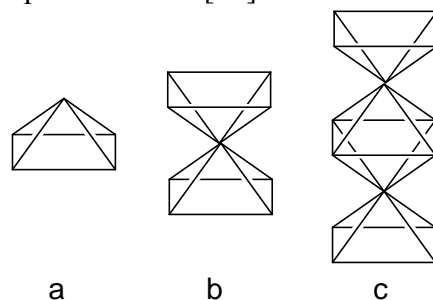
in the beginning, recent developments in this area have successfully revealed the general mechanism of formation of these finite sized molecular compounds. Recent advancements in this branch of lanthanide chemistry although still in its infancy, have successfully revealed the general mechanism of formation of these finite sized molecular entities [28]. When lanthanide salts, usually $[\text{LnX}_3 \cdot (\text{H}_2\text{O})_n]$ ($\text{X} = \text{Cl}, \text{I}, \text{NO}_3, \text{OTf}, \text{ClO}_4$), are hydrolyzed in the presence of a base (*e.g.* NaOH), they tend to form polynuclear oxo/hydroxo aggregates upon the condition that the extent of hydrolysis is carefully controlled. These clusters can either be formed from the bulk lanthanide salt [29-33] or in the presence of a suitable ligand (*e.g.* carboxylates, β -diketonates, alkoxides, phenoxides) [34-38]. In this context, the term “ligand-controlled hydrolysis“ is often used. However, the molecular structure of the final compound often remains unpredictable and unexpected; hence, unusual assemblies could be isolated and characterized.

1. Systematic Approach to Nanoscaled Lanthanide Clusters

In our previous studies we were mainly focused on the systematic approach to functionalized lanthanide oxo/hydroxo clusters [23, 35, 36, 39, 40]. Basically two different synthetic approaches were investigated. One way to obtain these compounds is the hydrolysis of moisture-sensitive starting material, whereas in the other approach the water molecules are deprotonated in a controlled way. The latter pathway involves the reaction of $[\text{LnCl}_3 \cdot (n \text{ H}_2\text{O})]$ and a suitable ligand in the presence of *e.g.* triethylamine as a base to give nanoscaled cluster compounds. Thereby the crystal water is deprotonated to give the hydroxo bridges. In the beginning of our research in this area we were mainly interested in understanding the formation of the clusters. Based on this fundamental knowledge, the research is meanwhile more focused on the functionality of the clusters.

1.1. Hydrolytic Pathway

By using the first approach, which implies the hydrolysis of a desolvated moisture-sensitive starting material like LnCl_3 , we reported on lanthanide clusters employing *o*-nitrophenolate as ligand some time ago [35, 36]. Tetradecanuclear nitrophenolate clusters of composition $[\text{Ln}_{14}(\mu_4\text{-OH})_2(\mu_3\text{-OH})_{16}(\text{o-O}_2\text{N-C}_6\text{H}_4\text{-O})_{24}]$ ($\text{Ln} = \text{Dy}$ (**1a**), Er (**1b**), Tm (**1c**), Yb (**1d**)) were isolated by us (Fig. 1). The Ln_{14} -core of **1a-d** can be described as a chain of three corners sharing lanthanide octahedra, in which one corner of the two outer octahedra is missing. The diameter of **1a-d** is about 2.06 nm. As also pointed out by other groups the structures of **1a-d** are based on a common structural motive in lanthanide chemistry [41]. **1a-d** can be considered as an assembly (or aggregate) of two nonanuclear clusters such as $[\text{Y}_9(\mu_4\text{-O})_2(\mu_3\text{-OH})_8(\text{aacac})_{16}]^-$ [42] (aacac = allyl acetatoacetate), and $[\text{Ln}_9(\mu_4\text{-O})_2(\mu_3\text{-OH})_8(\text{BA})_{16}]^-$ [41] (BA = benzoylacetone, $\text{Ln} = \text{Sm}, \text{Eu}, \text{Gd}, \text{Dy}, \text{Er}$), sharing their square based units (Scheme 1). The nonanuclear clusters themselves can be regarded as being composed of two square pyramidal $[\text{Ln}_5(\mu_4\text{-O})(\mu_3\text{-OH})_4]^{9+}$ units, which are sharing the apical lanthanide ion. Pentanuclear clusters such as $[\text{Eu}_5(\mu_4\text{-OH})(\mu_3\text{-OH})_4(\text{Ph}_2\text{acac})_{10}]$ (Ph_2acac = dibenzoylmethanide) have been reported earlier [43].



Scheme 1. Schematic chart of the pentanuclear $[\text{Ln}_5(\mu_4\text{-O})(\mu_3\text{-OH})_4]^{9+}$ unit (a), which can be considered as building block for nonanuclear (b) and tetradecanuclear clusters (c).

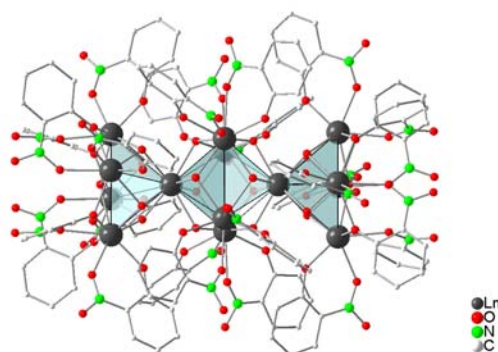


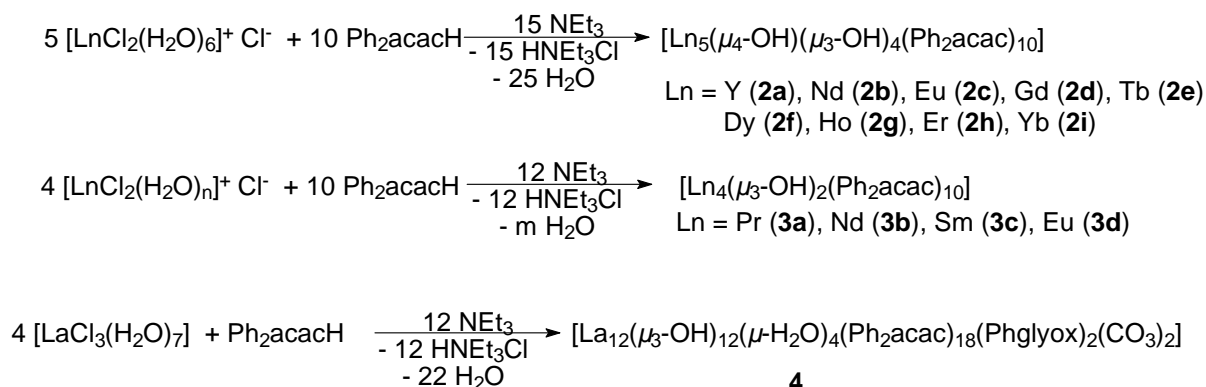
Fig.1: Solid-state structure of **1a-d** showing the atom labeling scheme, omitting hydrogen atoms (Ln = Dy, Er, Tm, Yb).

1.2. Reactions starting from $[\text{LnCl}_3 \cdot (n \text{ H}_2\text{O})]$

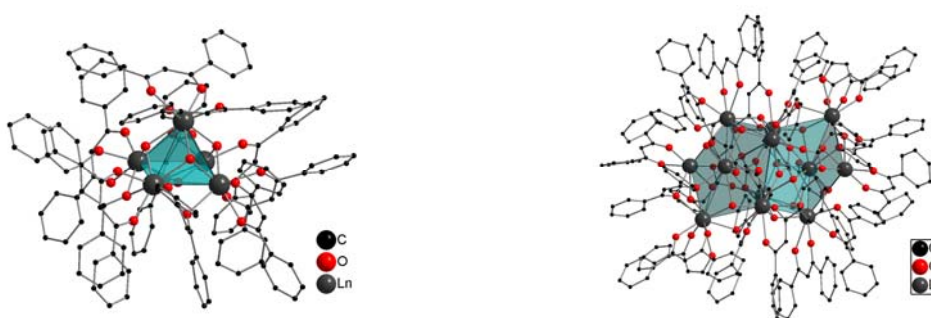
The disadvantages of the hydrolytic pathway are the relative low yields. To avoid this problem we and other groups started to use lanthanide trichloride hydrates $[\text{LnCl}_3 \cdot (n \text{ H}_2\text{O})]$, ($n = 6, 7$) as starting material. By using this approach, the crystal water molecules are deprotonated in a controlled fashion by a base giving oxo/hydroxo clusters in gram scale [27]. In general, the dimensions of the cage depend on the size of both the lanthanide ion and the ligand. In this context, we and others have reported on the synthesis and structure of pentanuclear lanthanide clusters $[\text{Ln}_5(\mu_4\text{-OH})(\mu_3\text{-OH})_4(\text{Ph}_2\text{acac})_{10}]$ (Ln = Y (**2a**), Nd (**2b**), Eu (**2c**), Gd (**2d**), Tb (**2e**), Dy (**2f**), Ho (**2g**), Er (**2h**), Yb (**2i**) (Fig. 2) [C1.5:3] [21, 27, 43, 44].(Lit.) The clusters were obtained by reacting $[\text{LnCl}_3 \cdot (6 \text{ H}_2\text{O})]$ with dibenzoylmethane (Ph_2acacH) in the presence of triethylamine (Scheme 2). In the square base face four lanthanide atoms are linked by one $\mu_4\text{-O}$ atom. In **2a-i** each lanthanide ion is coordinated to eight oxygen atoms displaying a square antiprismatic arrangement. The Ln_5 core is surrounded by ten peripheral Ph_2acac ligands. The ligand shows two types of coordination behaviour. Six ligands are terminal chelates and four are bridging chelates bonding to two metal ions that belong to the base of the polyhedron. The apical lanthanide atom, which lies on a fourfold symmetry axis, is bonding to two chelating ligands.

In contrast, by using the larger lanthanides and starting from $[\text{LnCl}_3 \cdot (n \text{ H}_2\text{O})]$ ($n = 6, 7$), tetranuclear lanthanide clusters of composition $[\text{Ln}_4(\mu_3\text{-OH})_2(\text{Ph}_2\text{acac})_{10}]$ (Ln = Pr (**3a**), Nd (**3b**), Sm (**3c**) and Eu (**3d**)) were obtained in a similar manner (Scheme 2) [40],[44]. Single crystal X-ray analyses of these compounds revealed that each cluster consists of four lanthanide atoms, two μ_3 -oxygen atoms, and ten Ph_2acac ligands, which make up the peripheral part of the cluster. Three types of coordination modes are observed for the Ph_2acac ligation to the metal centers, *i.e.* six Ph_2acac ligands coordinate in η^2 -, two further ones in $\mu\text{-}\eta^2$ - and the last two ones in $\mu\text{-}\eta^2\text{-}\eta^2$ -mode.

Applying the same reaction conditions but using the largest rare-earth metal lanthanum, the dodecanuclear hydroxy-bridged cluster $[\text{La}_{12}(\mu_3\text{-OH})_{12}(\mu\text{-H}_2\text{O})_4(\text{Ph}_2\text{acac})_{18}(\text{Phglyox})_2(\text{CO}_3)_2]$ (**4**) templated by CO_3^{2-} and phenylglyoxylate (Phglyox) was obtained (scheme 2) [45]. The solid state structure of the La_{12} -cluster is shown in Figure 2. The asymmetric unit comprises only half of the molecule, *i.e.* containing six lanthanum atoms, whereby the other half is generated by a centre of inversion. Each La^{3+} -ion is coordinated by nine oxygen atoms. The oxygen atoms either belong to hydroxy or water groups.



Scheme 2.

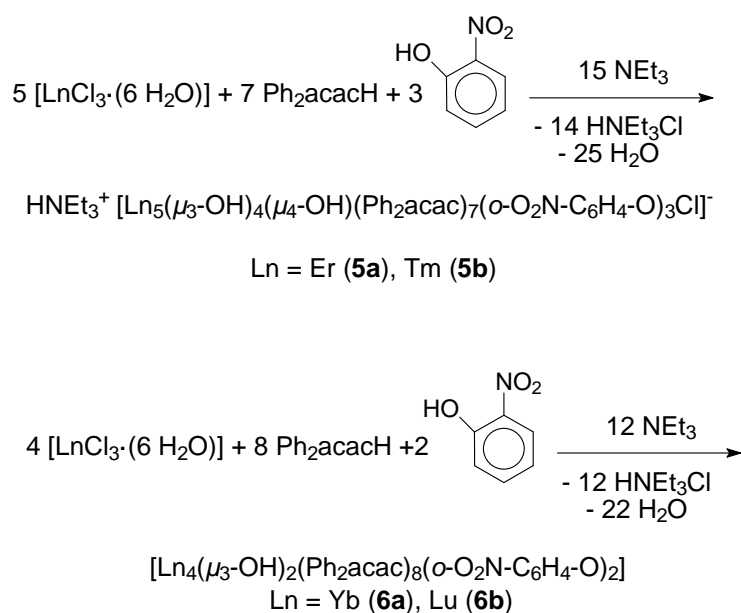
Fig.2: Solid state structure of **2a-i** (left, Ln = Y, Nd, Eu, Gd, Tb, Dy, Ho, Er, Yb) and **4** (right) showing the atom labeling scheme, omitting hydrogen atoms.

2. Functional Nanomaterials

In contrast to many chalcogenide clusters of the *d*- and *f*-elements, the presented compounds cannot only be made in large scale but they are also tremendously stable in the solid state and in solution, as shown by pulsed gradient spin-echo (PGSE) diffusion experiments (see below). All compounds are air and moisture stable and are not decomposed by various bases. As a result of these properties, we were interested in studying the properties of the clusters. Beside the physical properties such as luminescence and magnetism we were also interested in attaching chemical functional groups onto the outer ligand shell of the cluster.

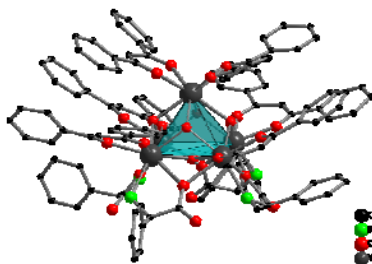
2.1. Chemical Functionalization

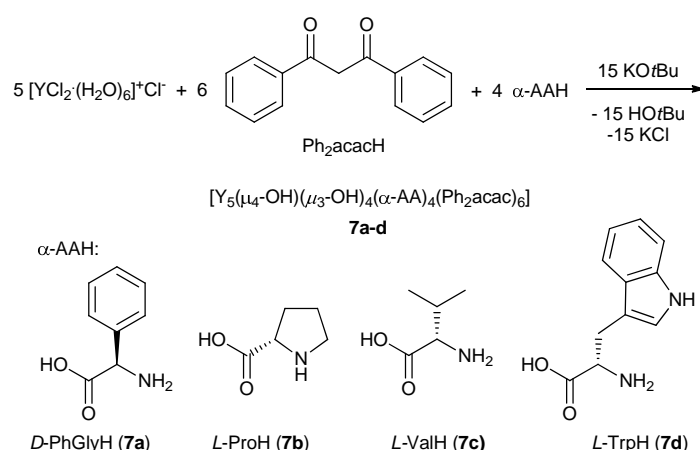
To introduce functionality into the lanthanide oxo/hydroxo clusters, we started to synthesize clusters with two different ligands. Within a first attempt, we used our standard ligands dibenzoylmethane and *o*-nitrophenol as well as the trichloride hydrates of the rather small lanthanides to obtain ionic clusters of composition $\text{HNEt}_3^+[\text{Ln}_5(\mu_3\text{-OH})_4(\mu_4\text{-OH})(\text{Ph}_2\text{acac})_7(\text{o-O}_2\text{N-C}_6\text{H}_4\text{-O})_3\text{Cl}]^-$ (Ln = Er (**5a**), Tm (**5b**)) (Scheme 4) [39]. In contrast, by using the even smaller center metals Yb and Lu, clusters of composition $[\text{Ln}_4(\mu_3\text{-OH})_2(\text{Ph}_2\text{acac})_8(\text{o-O}_2\text{N-C}_6\text{H}_4\text{-O})_2]$ (Ln = Yb (**6a**), Lu (**6b**)) were isolated (Scheme 3). A comparison between the new mixed dibenzoylmethanide/*o*-nitrophenolate clusters and pure dibenzoylmethanide clusters shows an interrelation. The dibenzoylmethanide ligands, which act in the pure dibenzoylmethanide clusters as chelating and bridging ligands binding in a $\mu\text{-}\eta^2$ -mode are formally replaced by the *o*-nitrophenolates. Thus, by using this synthetic approach we can now selectively substitute dibenzoylmethanide by other ligands on a fixed position of the cluster.



Scheme 3.

Based on these considerations we started to incorporate molecules with more chemical functionalities into the ligand sphere of the clusters [C1.5:5], whereby α -amino acids turned out to be ideal ligands [39, 46]. They can be incorporated in the ligand sphere of a pentanuclear cluster by reacting $[\text{YCl}_2(\text{H}_2\text{O})_6]^+\text{Cl}^-$ with dibenzoylmethane and the corresponding α -amino acid in presence of a base to give four mixed-ligated pentanuclear yttrium hydroxo clusters $[\text{Y}_5(\mu_4\text{-OH})(\mu_3\text{-OH})_4(\alpha\text{-AA})_4(\text{Ph}_2\text{acac})_6]$ ($\alpha\text{-AA} = D$ -phenyl glycine (**7a**), *L*-proline (**7b**), *L*-valine (**7c**), and *L*-tryptophan (**7d**)). In contrast to our previous studies, we used potassium *tert*-butoxide instead of triethylamine as base. Thus we preemptively avoided the formation of triethylammonium chloride, which turned out to be poorly removable from the products in the crystallization step. The solid state structures of all compounds were established by single crystal X-ray diffraction (Fig. 3). In these enantiomerically pure chiral clusters the dibenzoylmethanide and amino acid ligands are accommodated in the coordination spheres of the yttrium atoms. In compounds **7a-d**, the six η^2 -coordinating chelating dibenzoylmethanide ligands remain in the same terminal positions as compared to the pure dibenzoylmethanide clusters $[\text{Ln}_5(\mu_4\text{-OH})(\mu_3\text{-OH})_4(\text{Ph}_2\text{acac})_{10}]$ (**2a-i**). In clusters **7a-d**, the four bridging and chelating $\mu\text{-}\eta^2$ -coordinating dibenzoylmethanide ligands are now formally substituted by the amino acids, acting as coligands. The specific optical rotations of all four compounds were determined. PGSE NMR diffusion measurements as a function of concentration have been carried out on the model cluster **7c**, giving the first unambiguous evidence for these lanthanide oxo/hydroxo clusters being stable in solution.

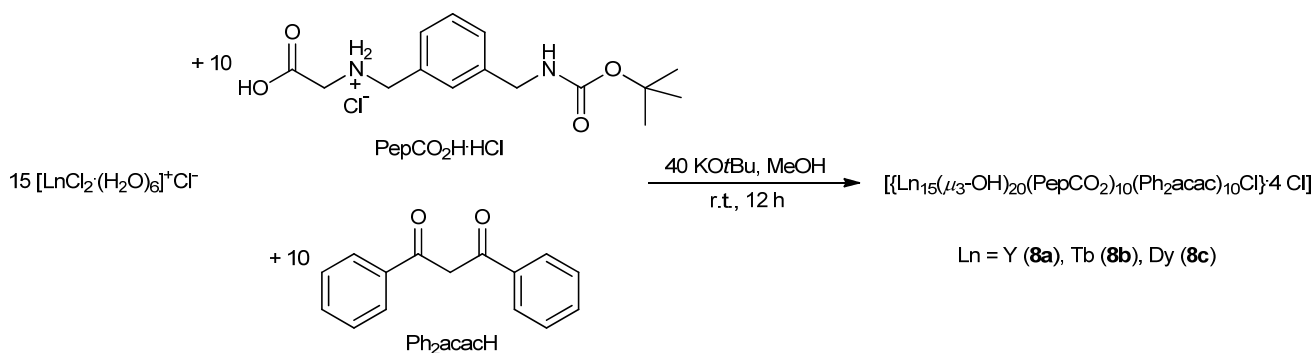
Figure 3: Solid-state structure of yttrium phenylglycine cluster **7a**.



Scheme 4.

The next aim was the introduction of the lanthanide oxo/hydroxo clusters into the biosphere. Based on compounds **7a-d**, there two synthetic pathways to reach this goal. The first route would be the formation of a peptide chain starting from compounds **7a-d**. As an alternative, a peptide or a similar reagent is anchored during the cluster synthesis onto the lanthanide atoms. In cooperation with the research group of Prof. Bräse we applied the second method to obtain cell penetrating clusters. In this case peptoids instead of peptides were used. Peptoids are oligo-*N*-alkyl glycines and are very similar to native peptides. Peptoids are stable against proteases *in vivo* and *in vitro*, have antibiotic properties and can bind to receptors or proteins [47].

Reaction of the peptoid 2-[3-(((*tert*-butoxycarbonyl)amino)methyl)benzyl]amino]acetic acid hydrochloride ($\text{PepCO}_2\text{H}\cdot\text{HCl}$) with $[\text{LnCl}_3\cdot(\text{H}_2\text{O})_6]$ ($\text{Ln} = \text{Y}, \text{Tb}, \text{Dy}$) and dibenzoylmethane (Ph_2acacH) in the presence of potassium *tert*-butoxide in methanol resulted in the pentadecanuclear rare-earth metal hydroxy cluster $[\{\text{Ln}_{15}(\mu_3\text{-OH})_{20}(\text{PepCO}_2)_{10}(\text{Ph}_2\text{acac})_{10}\text{Cl}\}\cdot 4 \text{Cl}]$ ($\text{Ln} = \text{Y}$ (**8a**), Tb (**8b**), Dy (**8c**)) (Scheme 5) in up to 55 % single crystalline yield.



Scheme 5.

All compounds are available in gram scale and were characterized by standard analytical and spectroscopic techniques and the solid state structures were determined by single crystal X-ray diffraction (Fig. 4). The $[\{\text{Ln}_{15}(\mu_3\text{-OH})_{20}(\text{PepCO}_2)_{10}(\text{Ph}_2\text{acac})_{10}\text{Cl}\}]^{4+}$ cation consists of five $\{\text{Ln}_4(\mu_3\text{-OH})_4\}^{8+}$ heterocubane subunits, which are fused to a ring structure exhibiting an edge-sharing arrangement. The cyclic shape of this rare-earth metal hydroxide scaffold is additionally stabilized by a centered μ_5 -bridging chloro atom displaying pentagonally shaped lanthanide moieties. The ten Ph_2acac ligands uniformly coordinate in a chelating η^2 -mode one of those ten

rare-earth metal atoms each, which do not act as linking points between adjacent heterocubane subunits and are coplanarly aligned with respect to the pentagonal rings. In contrast, the PepCO_2 ligands uniformly act as tridentate ligands and are perpendicularly aligned to the pentagonal rings. Each ligand coordinates with both carboxylate oxygen atoms and the glycinic nitrogen atom to three metal centers. Although a similar central structural core $\{\text{Ln}_{15}(\mu_3\text{-OH})_{20}\text{Cl}\}^{24+}$ has been reported [34, 48], a coordination of peptoids to an inorganic core is to the best of our knowledge unique. To investigate the stability in solution, ESI-MS spectra of compounds **1-3** were recorded in different solvents. For all compounds the $[\{\text{Ln}_{15}(\mu_3\text{-OH})_{20}(\text{PepCO}_2)_{10}(\text{Ph}_2\text{acac})_{10}\text{Cl}\} \cdot 2\text{Cl}]^{2+}$ cation could be clearly detected from methanol, ethanol, propanol and DMF (Fig. 5). Furthermore, PGSE measurements also confirmed the stability of such clusters, which was exemplified for the diamagnetic compound **8a**.

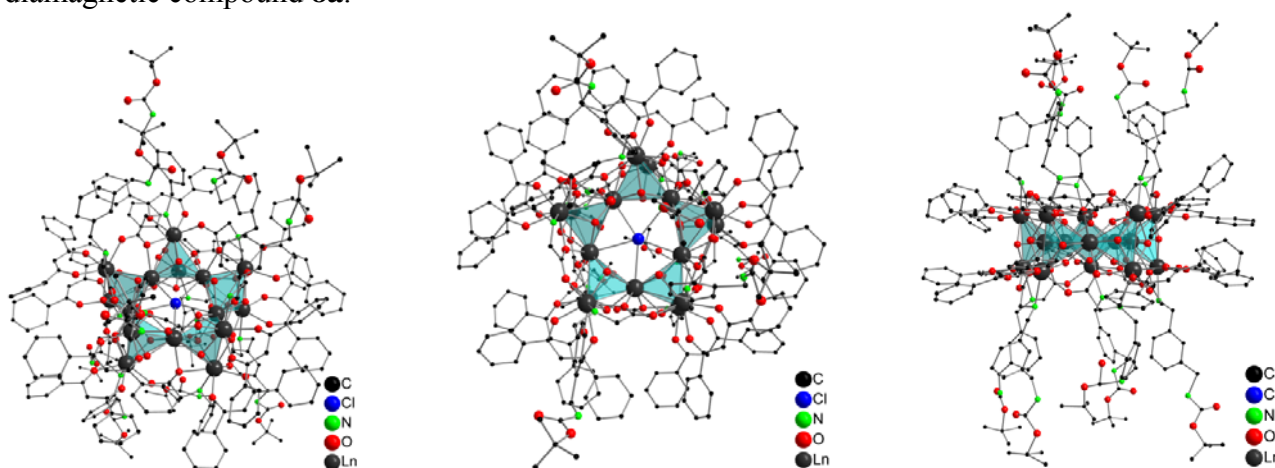


Fig.4. Solid state structure of **8a-c**. Left: front view. Middle: top view. Right: side view. Hydrogen atoms are omitted for clarity.

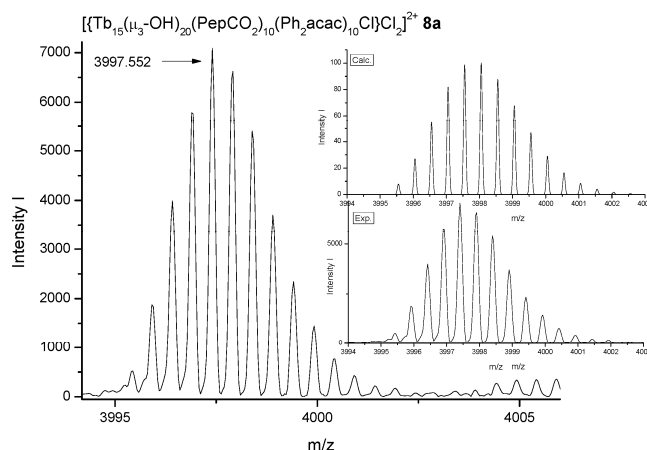


Fig.5. FTICR-ESI-MS spectrum of dicationic species $[\{\text{Tb}_{15}(\mu_3\text{-OH})_{20}(\text{PepCO}_2)_{10}(\text{Ph}_2\text{acac})_{10}\text{Cl}\} \text{Cl}_2]^{2+}$ derived from compound **8b** from a methanol solution including comparison between calculated and experimentally determined spectra.

2.2. Physical Properties – Luminescence and Magnetism

a) Luminescence

In cooperation with other groups (K. Landfester and C. K. Weiss, Mainz; C. Wickleder, Siegen) the clusters **2b**, **3a**, and **3c** were used in various polymer matrices via miniemulsion polymerization is presented [C1.5:7] [49]. The resulting cluster-polymer hybrid nanoparticles are spherical in shape

and possess a narrow size distribution as investigated by photon cross correlation spectroscopy (PCCS) and transmission electron microscopy (TEM). The exact Ln-content in the nanoparticles was exemplarily investigated for Eu- and Nd-containing polymer dispersions via inductively coupled plasma-optical emission spectrometry (ICP-OES). As a result of encapsulation, more than $1000 \text{ mg}\cdot\text{L}^{-1}$ of the hydrophobic lanthanide clusters could successfully be dispersed in water. The photophysical properties of the emulsion show the successful avoidance of water from the vicinity of the clusters. Furthermore, a very efficient energy transfer from the ligand and polymeric unit to Eu^{3+} -ions can be observed in dispersion. Based on the different glass transition temperatures (T_g) of the applied polymers, monolayers of the nanoparticles and efficient luminescent thin polymer films were obtained by spin coating (Fig. 6).



Fig.6: Luminescence of the **2b** in a matrix of polylaurylmethacrylate (PLMA).

Luminescence investigations (with the group of Prof. Bräse) of the Tb-cluster **8c** have revealed its propensity to provide LMCT-induced photoluminescence. The combination of the three ligands (μ_3 -OH, Ph_2acac and PepCO_2) and the coordination geometry of Tb^{3+} -ions as a result of the structural motif obtained have facilitated a favored emission from the excited $^5\text{D}_4$ into the $^7\text{F}_3$ ground state of the Tb^{3+} -ions. As a result, the rare case of orange photoluminescence at 613 nm has been observed, as proven *via* time-resolved emission spectra. Moreover the absence of solvent-based high-energy C-H-stretch vibrations in THF- d_8 has confirmed the avoidance of quenching of the photoluminescence observed. Higher luminescence intensities and longer lifetimes of excited states compared to usage of non-deuterated THF have reflected this issue.

b) Magnetism

In cooperation with the group of Prof. Powell the magnetic properties of some compounds were determined [C1.5:3, C1.5:4]. Although the study of paramagnetic metal-ion aggregates has been of increasing interest in attempts to assemble single molecule magnets (SMMs) little work has been reported on purely lanthanide-based systems. In this context some hydroxo-bridged dysprosium triangles showing SMM behavior of thermally excited spin states were reported very recently [23]. It should be noted that dysprosium(III) shows manifold magnetic behavior and was the first known example of the so called “spin ice” effect [50]. Both static (dc) and dynamic (ac) magnetic properties of the dysprosium cluster **2f** have been studied [21]. The temperature-dependent ac susceptibilities of this compound were measured under zero dc field. Below 3 K the appearance of slow relaxation of the magnetization typical for single molecule magnets is seen, even if no hysteresis effects on the M vs H data is observed above 1.8 K (Fig. 7).

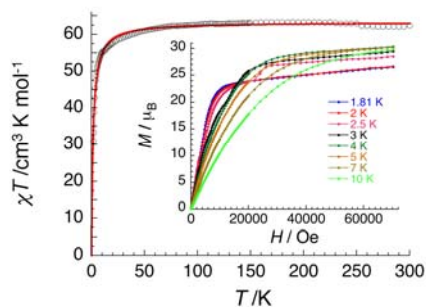


Fig.7: Temperature dependence of magnetic susceptibility at 1000 Oe and field dependence of the magnetization at low temperatures (inset) for **2c**.

Also for compound **8c** both static and dynamic magnetic properties have been studied, whereby the course of the χT product as a function of temperature features **8c** to be a ferromagnetic cluster compound. The appearance of slow relaxation of the magnetization below a temperature of 8 K may be attributed to **8c** being a SMM. Both the frequency-dependent in-phase and out-of-phase signals do not pass through maxima, suggesting that this compound is a SMM (Fig. 8). However, for compound **8c** this behaviour is associated with a blocking temperature below 1.8 K, even at a frequency of 1500 Hz.

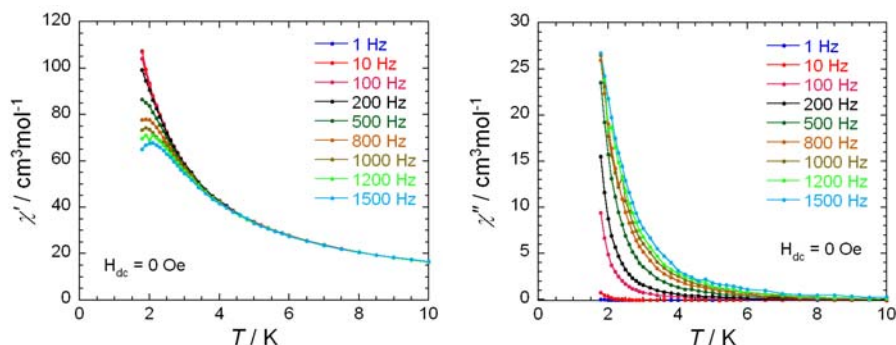


Fig.8: Susceptibility measurements of **8c** as a function of temperature when applying alternate current.

2.3. *In vitro* investigations

Well defined clusters of the rare-earth metals have hitherto not been used for any biological application. Based on this consideration we were interested in synthesizing rare-earth metal based clusters having suitable luminescent properties for various *in vitro* experiments. To reach this goal, the anchoring of a cell penetrating agent onto a structurally well defined rare-earth metal cluster is necessary. The peptoid ligand PepCO₂ (see 2.1) was originally developed and designed for accessing cellular systems. Thus, within this project cluster compounds **8a-c** ought to generate a species which unifies rare earth metals' valuable photophysical properties and peptoid ligand's biorelevant chemical properties to provide novel bioaccessible and –compatible structures on the molecular scale.

In cooperation with the group of Dr. Schepers HeLa cells were treated with clusters **8a-c**. Confocal live imaging experiments have revealed an internalization process of the clusters into the cells, although only little amounts could enter the cells due to their restricted solubility in aqueous media. A HeLa cell is a cell type in an immortal cell line used in scientific research; amongst which it depicts one of the oldest and most commonly used human cell lines [51]. The cell-derived

fluorescence is rather weak compared to that of the cluster compounds, which are apparently enriched in the endoplasmic reticulum. The yttrium based cluster **8a** provides much more intense fluorescence than its terbium and dysprosium analogues **8b** and **8c**; and it already glares dark blue when irradiated with a fluorescent lamp. Excitation of **8a** with a UV laser ($\lambda = 368$ nm) effectuates a bathochromic shift of emission, *i.e.* to higher wavelengths ($\lambda = 482$ - 571 nm) [52]. The light yield of **8a** is strikingly higher than for **8b** and **8c**, however, all the clusters are insoluble in water and undergo precipitation when incubated with cells. As a consequence, concentrations above $10 \mu\text{M}$ enhance the toxicity of **8a-c** explicitly. The luminescence of terbium cluster **8b** comprises a wider range of wavelengths ($\lambda = 482$ - 696 nm), and in contrast to **8a** and **8c**, it is enriched in both the cytosol and cell nucleus (Fig. 9).

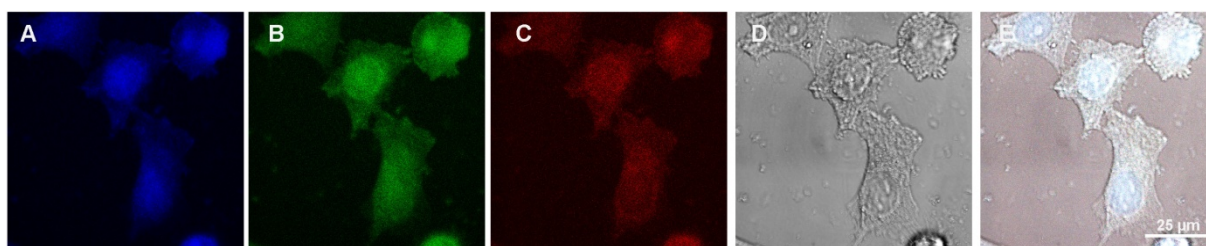


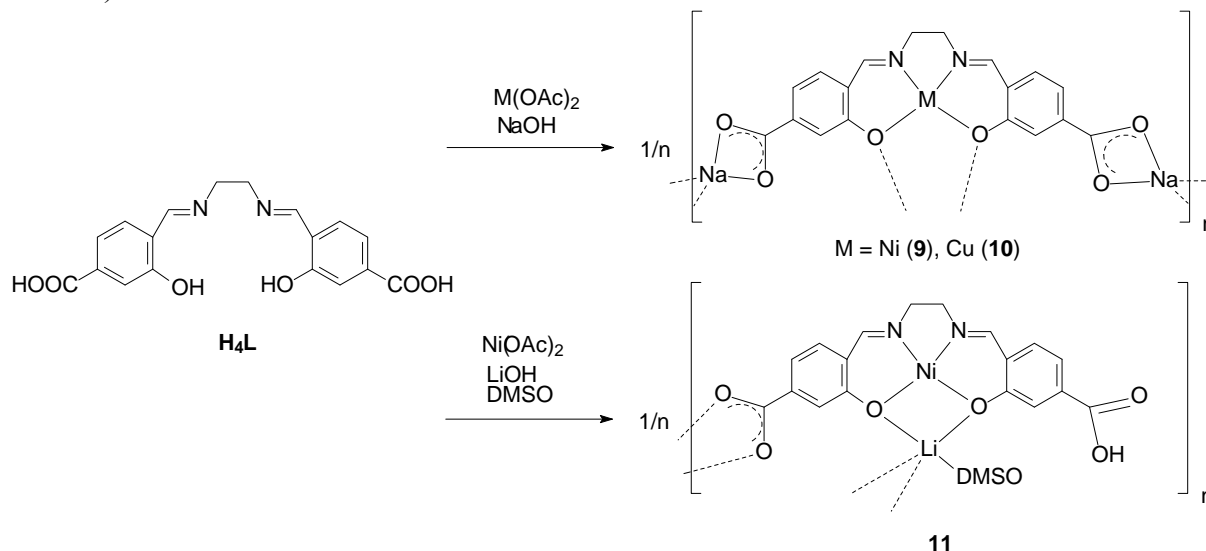
Fig.9: Images of HeLa cells incubated with cluster **8c**. The left box A presents the emission enquiry ranging from $\lambda = 380$ - 474 nm, the second box B presents the emission enquiry ranging from $\lambda = 499$ - 552 nm, the third box C presents the emission enquiry ranging from $\lambda = 581$ - 696 nm, whereby the fourth box D shows the phase contrast and the right box E shows the overlap of the former three emission ranges.

3. Metal–organic frameworks (MOFs) and infinite coordination polymers (ICPs)

In the second part of the project we are dealing with lanthanide based metal–organic frameworks (MOFs) and infinite coordination polymers (ICPs). The synthesis of MOFs requires two main components: rigid bifunctional organic linkers and metal centers. The rigid bifunctional organic linkers serve to bridge the metal centers, whereas the metal centers act as nodes and as specified connectivities in the resulting MOF architecture [4]. In most cases the metal centers used have been $3d$ metals such as zinc [4], but there have also some lanthanide based MOFs been reported [5, 53, 54]. Whereas in most MOF materials rigid organic molecules are used as linkers, there are also some examples in the literature in which the use of “metalloligands” is demonstrated [2, 6, 7, 55-57]. In this approach, functionalized ligands (L) coordinate to a metal center (M) forming a “metalloligand” (ML) which is suitable for the construction of higher dimensional homo- or heterometallic ICP’s or MOF’s through reaction with further metal centers. Interest in such “metalloligands” stems from the fact that metal ions can have an unsaturated coordination sphere, which could be used for hydrogen storage *via* chemisorptions [6]. Another potential application is homogeneous catalysis [58, 59]. The “metalloligands” [η^6 -1,4-benzene dicarboxylate) $\text{Cr}(\text{CO})_3$] [60], functionalized salphen (N,N' -phenylenebis(salicylideneimine)) templates [61], and functionalized salen (N,N' -bis(salicylidene)ethylenediamine) ligands have been reported [62]. In this context some ICP’s and MOF’s consisting of salen-based “metalloligands” with additional functional groups such as carboxylates [61], pyridyl groups [59], and benzoic acid groups [63] in *para*-position to the OH group have been published.

Bearing this in mind, we used N,N' -bis(4-carboxysalicylidene)ethylenediamine (**H₄L**) as a salen ligand [64], which has carboxylate groups in *meta*-position to the OH groups [65]. As a result of the different stereochemistry compared to the established systems and the resulting different angles, we expected a significant influence on the shape of the ICP [C1.5:4]. Surprisingly no polymeric

structures using **H₄L** as ligand were reported so far. Reaction of **H₄L** with nickel or copper acetate in the presence of sodium hydroxide in DMF resulted after crystallization in the ICP $[\text{Na}_4(\text{LM})_2 \cdot (\text{H}_2\text{O})_9]_n$ ($\text{M} = \text{Ni}$ (**9**), Cu (**10**)) (Scheme 6). Compound **9** and **10** were obtained as isostructural 2D ICPs. In contrast to these results, the reaction of compound **H₄L** with nickel acetate in the presence of lithium hydroxide in DMSO resulted in the polymeric one 1D ICP $[(\text{DMSO})\text{Li}\{(\text{HL})\}\text{Ni}]_n$ (**11**) (Scheme 6).



Scheme 6.

The shape of the coordination polymers depends on the alkaline metal used, which is coordinated to the carboxylate function. A thermal study shows that compounds **9** and **10** are very robust. Additionally, for the copper compound a weak antiferromagnetic interaction was observed.

Treatment of a DMF/water solution of compound **9** with $[\text{Ln}(\text{NO}_3)_3 \cdot (\text{H}_2\text{O})_n]$ ($\text{Ln} = \text{Er}$ ($n = 5$), Lu ($n = 4$)) resulted after work-up and crystallization in the polymeric lanthanide-nickel compounds $[\{\text{Ln}_2(\text{LNi})_3(\text{DMF})(\text{H}_2\text{O})_3\} \cdot (\text{DMF})_4 \cdot (\text{H}_2\text{O})_{10}]_n$ ($\text{Ln} = \text{Er}$ (**12**), Lu (**13**)) (Scheme 7, Fig. 10) [C1.05:10]. Compounds **12** and **13** were obtained as red crystals. The structures of **12** and **13** result from the influence of two different secondary building units (SBUs). One SBU can be regarded as a distorted octahedron made up by two lanthanide ions bridged by four carboxylates. The second SBU is a distorted hexagon. Reaction of *in situ* prepared compound **9** in DMSO / THF with an aqueous solution of dysprosium nitrate resulted in the polymeric dysprosium-nickel compound $[\text{Dy}\{(\text{LNi})(\text{DMSO})(\text{NO}_3)\}(\text{H}_2\text{O})_2 \cdot (\text{DMSO})]_n$ (**14**) (Scheme 7). In contrast to compounds **2** and **3**, only one SBU is formed by a $[\text{Dy}_2(\mu\text{-O}_2\text{CR})_2(\eta^2\text{-O}_2\text{CR})_2]$ building block. This SBU consists of a parallelogram having only four points of extension [5].

Magnetic studies on compound **12** and **14** were performed in the group of Prof. Powell using a SQUID magnetometer operating in the 1.8-300 K temperature range with applied magnetic field of 0.1 T. These magnetic susceptibility measurements under zero dc field showed that the nickel-dysprosium compound **14** exhibits a non-zero frequency dependence of out-of-phase components below 12 K indicating slow relaxation of its magnetization under these conditions. The presented strategy now offers a wide area in which the *3d* metal as well as the *4f* metal can be varied.

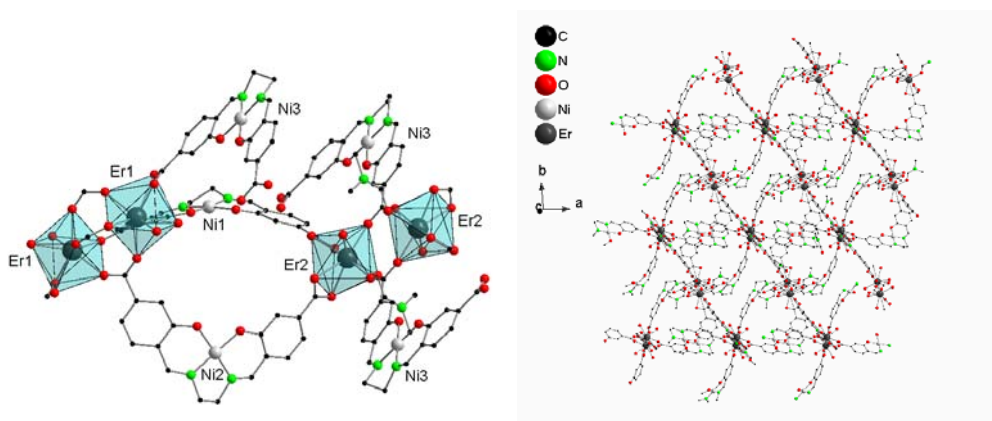
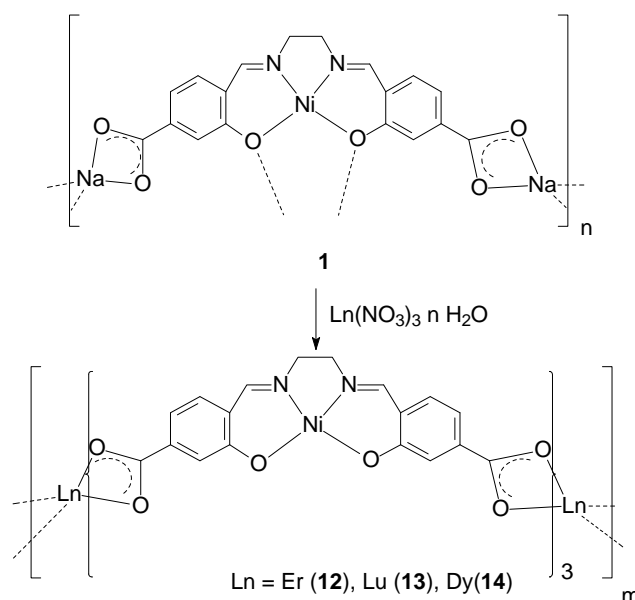


Fig.10: Solid state structure of **12**, omitting hydrogen atoms. Left: asymmetric unit. Right: cutout of the polymeric structure. Compound **13** is isostructural to **12**.



Scheme 7.

References

- [1] M. Oh, and C.A. Mirkin, *Nature*, **438**, 651, (2005).
- [2] A.M. Spokoyny, D. Kim, A. Sumrein, and C.A. Mirkin, *Chem. Soc. Rev.*, **38**, 1218, (2009).
- [3] R. Robson, *Dalton Transactions*, 5113, (2008).
- [4] O.M. Yaghi, M. O'Keeffe, N.W. Ockwig, H.K. Chae, M. Eddaoudi, and J. Kim, *Nature*, **423**, 705, (2003).
- [5] D.J. Tranchemontagne, J.L. Mendoza-Cortes, M. O'Keeffe, and O.M. Yaghi, *Chem. Soc. Rev.*, **38**, 1257, (2009).
- [6] M. Dinca, and J.R. Long, *Angew. Chem., Int. Ed. Engl.*, **47**, 6766, (2008).
- [7] J. Lee, O.K. Farha, J. Roberts, K.A. Scheidt, S.T. Nguyen, and J.T. Hupp, *Chem. Soc. Rev.*, **38**, 1450, (2009).
- [8] S. Qiu, and G. Zhu, *Coord. Chem. Rev.*, **253**, 2891, (2009).
- [9] X.-M. Zhang, Z.-M. Hao, W.-X. Zhang, and X.-M. Chen, *Angew. Chem. Int. Ed.*, **46**, 3456, (2007).

- [10] M.D. Allendorf, C.A. Bauer, R.K. Bhakta, and R.J.T. Houk, *Chem. Soc. Rev.*, **38**, 1330, (2009).
- [11] Z. Li, G. Zhu, X. Guo, X. Zhao, Z. Jin, and S. Qiu, *Inorg. Chem.*, **46**, 5174, (2007).
- [12] Q.-R. Fang, G.-S. Zhu, M. Xue, Q.-L. Zhang, J.-Y. Sun, X.-D. Guo, S.-L. Qiu, S.-T. Xu, P. Wang, D.-J. Wang, and Y. Wei, *Chem. Eur. J.*, **12**, 3754, (2006).
- [13] Z. Zheng, *Chem. Commun.*, 2521, (2001).
- [14] Z. Zheng, in K.A. Gschneidner Jr., J.-C.G. Bünzli and V.K. Pecharsky (Editors), *Handbook on the Physics and Chemistry of Rare Earths Elements*, Vol. 40, Elsevier, Amsterdam, 2010, p. 109.
- [15] S. Banerjee, G.A. Kumar, R.E. Riman, T.J. Emge, and J.G. Brennan, *J. Am. Chem. Soc.*, **129**, 5926, (2007).
- [16] D. Gatteschi, A. Caneschi, L. Pardi, and R. Sessoli, *Science*, **265**, 1054, (1994).
- [17] W. Wernsdorfer, in D. Sellmyer and R. Skomski (Editors), *Advanced Magnetic Nanostructures*, Springer US, 2006, p. 147.
- [18] R. Winpenny, G. Aromí, and E. Brechin, *Struct. Bonding*, **122**, 1, (2006).
- [19] R. Winpenny, J.-N. Rebilly, and T. Mallah, *Struct. Bonding*, **122**, 103, (2006).
- [20] O. Poncelet, W.J. Sartain, L.G. Hubert-Pfalzgraf, K. Folting, and K.G. Caulton, *Inorg. Chem.*, 263, (1989).
- [21] M.T. Gamer, Y. Lan, P.W. Roesky, A.K. Powell, and R. Clerac, *Inorg. Chem.*, **47**, 6581, (2008).
- [22] N. Mahé, O. Guillou, C. Daignebonne, Y. Gérard, A. Caneschi, C. Sangregorio, J.Y. Chane-Ching, P.E. Car, and T. Roisnel, *Inorg. Chem.*, **44**, 7743, (1995).
- [23] J. Tang, I. Hewitt, N.T. Madhu, G. Chastanet, W. Wernsdorfer, C.E. Anson, C. Benelli, R. Sessoli, and A.K. Powell, *Angew. Chem. Int. Ed.*, **45**, 1729, (2006).
- [24] T. Kajiwara, K. Katagiri, M. Hasegawa, A. Ishii, M. Ferbinteanu, S. Takaishi, T. Ito, M. Yamashita, and N. Iki, *Inorg. Chem.*, **45**, 4880, (1996).
- [25] A. Kornienko, T.J. Emge, G.A. Kumar, R.E. Riman, and J.G. Brennan, *J. Am. Chem. Soc.*, **122**, 3501, (2005).
- [26] L.-Z. Zhang, W. Gu, B. Li, X. Liu, and D.-Z. Liao, *Inorg. Chem.*, **46**, 622, (2007).
- [27] P.W. Roesky, G. Canseco-Melchor, and A. Zulys, *Chem. Commun.*, 738, (2004).
- [28] R. Wang, H. Liu, M.D. Carducci, T. Jin, C. Zheng, and Z. Zheng, *Inorg. Chem.*, **40**, 2743, (2001).
- [29] R. Wang, M.D. Carducci, and Z. Zheng, *Inorg. Chem.*, **39**, 1836, (2000).
- [30] Z. Zák, P. Unfried, and G. Giester, *J. Alloys Compd.*, **205**, 235, (1994).
- [31] G. Giester, P. Unfried, and Z. Zák, *J. Alloys Compd.*, **257**, 175, (1997).
- [32] A.-V. Mudring, T. Timofte, and A. Babai, *Inorg. Chem.*, **45**, 5162, (2006).
- [33] A. Babai, and A.-V. Mudring, *Z. Anorg. Allg. Chem.*, **632**, 1956, (2006).
- [34] R. Wang, Z. Zheng, T. Jin, and R.J. Staples, *Angew. Chem. Int. Ed.*, **38**, 1813, (1999).
- [35] M.R. Bürgstein, M.T. Gamer, and P.W. Roesky, *J. Am. Chem. Soc.*, **126**, 5213, (2004).
- [36] M.R. Bürgstein, and P.W. Roesky, *Angew. Chem. Int. Ed.*, **39**, 549, (2000).
- [37] M. Addamo, G. Bombieri, E. Foresti, M.D. Grillone, and M. Volpe, *Inorg. Chem.*, **43**, 1603, (2004).
- [38] L.G. Hubert-Pfalzgraf, L. Cauro-Gamet, A. Brethon, S. Daniele, and P. Richard, *Inorg. Chem. Commun.*, **10**, 143, (2007).
- [39] S. Datta, V. Baskar, H. Li, and P.W. Roesky, *Eur. J. Inorg. Chem.*, 4216, (2007).
- [40] V. Baskar, and P.W. Roesky, *Z. Anorg. Allg. Chem.*, **631**, 2782, (2005).
- [41] G. Xu, Z.-M. Wang, Z. He, Z. Lü, C.-S. Liao, and C.-H. Yan, *Inorg. Chem.*, **41**, 6802, (2002).
- [42] L.G. Hubert-Pfalzgraf, N. Miele-Pajot, R. Papiernik, and Jacqueline Vaissermann, *J. Chem. Soc., Dalton Trans.*, 4127, (1999).

- [43] R.-G. Xiong, J.-L. Zuo, Z. Yu, X.-Z. You, and W. Chen, *Inorg. Chem. Commun.*, **2**, 490, (1999).
- [44] P.C. Andrews, T. Beck, B.H. Fraser, P.C. Junk, M. Massi, B. Moubaraki, K.S. Murray, and M. Silberstein, *Polyhedron*, **28**, 2123, (2009).
- [45] P.C. Andrews, T. Beck, C.M. Forsyth, B.H. Fraser, P.C. Junk, M. Massi, and P.W. Roesky, *Dalton Transactions*, 5651, (2007).
- [46] D.T. Thielemann, I. Fernandez, and P.W. Roesky, *Dalton Transactions*, **39**, 6661, (2010).
- [47] S.M. Miller, R.J. Simon, S. Ng, R.N. Zuckermann, J.M. Kerr, and W.H. Moos, *Bioorg. Med. Chem. Lett.*, **4**, 2657, (1994).
- [48] R. Wang, H.D. Selby, H. Liu, M.D. Carducci, T. Jin, Z. Zheng, J.W. Anthis, and R.J. Staples, *Inorg. Chem.*, **41**, 278, (2002).
- [49] C. P. Hauser, D. T. Thielemann, M. Adlung, C. Wickleder, P. W. Roesky, C. K. Weiss, and K. Landfester, *Macromol. Chem. & Phys.*, accepted, (2011).
- [50] A.P. Ramirez, A. Hayashi, R.J. Cava, R. Siddharthan, and B.S. Shastry, *Nature*, **399**, 333, (1999).
- [51] R. Rahbari, T. Sheahan, and V. Modes, *BioTechniques*, **46**, 277, (2009).
- [52] K. Nassau, *The Physics and Chemistry of Colour: The Fifteen Causes of Colour*, Wiley & Sons, New York, 2001.
- [53] F. Luo, and S.R. Batten, *Dalton Transactions*, **39**, 4485, (2010).
- [54] D.-L. Long, A.J. Blake, N.R. Champness, C. Wilson, and M. Schröder, *J. Am. Chem. Soc.*, **123**, 3401, (2001).
- [55] M. Oh, and C.A. Mirkin, *Angew. Chem., Int. Ed. Engl.*, **45**, 5492, (2006).
- [56] X. Liu, *Angew. Chem., Int. Ed. Engl.*, **48**, 3018, (2009).
- [57] M.D. Hobday, and T.D. Smith, *Coord. Chem. Rev.*, **9**, 311, (1973).
- [58] E.M. McGarrigle, and D.G. Gilheany, *Chem. Rev.*, **105**, 1563, (2005).
- [59] S.-H. Cho, B. Ma, S.T. Nguyen, J.T. Hupp, and T.E. Albrecht-Schmitt, *Chem. Commun.*, 2563, (2006).
- [60] S.S. Kaye, and J.R. Long, *J. Am. Chem. Soc.*, **130**, 806, (2007).
- [61] S. Jung, and M. Oh, *Angew. Chem., Int. Ed. Engl.*, **47**, 2049, (2008).
- [62] S.J. Wezenberg, and A.W. Kleij, *Angew. Chem. Int. Ed.*, **47**, 2354, (2008).
- [63] Y.-M. Jeon, J. Heo, and C.A. Mirkin, *J. Am. Chem. Soc.*, **129**, 7480, (2007).
- [64] S.N. Poddar, *Z. Anorg. Allg. Chem.*, **322**, 326, (1963).
- [65] A. Bhunia, P.W. Roesky, Y. Lan, G.E. Kostakis, and A.K. Powell, *Inorg. Chem.*, **48**, 10483, (2009).